

# THE INVISCID PRIMITIVE EQUATIONS FOR THE OCEANS AND THE ATMOSPHERE: THEORETICAL AND COMPUTATIONAL ISSUES

Roger Temam

*Indiana University, Bloomington*

<http://mypage.iu.edu/~temam/>

## Collaborations

- ▶ J. Tribbia (NCAR)
- ▶ Q. Chen, M.-C. Shiue and A. Rousseau

## Articles

- ▶ A. Rousseau, R.T., J. Tribbia, [RTT08], *J. de Math. Pures et Appl.*, 2008.
- ▶ Q. Chen, M.-C. Shiue, and R.T., [CST09], The zero-mode of the inviscid Primitive Equations, *J. Scient. Computing*, to appear.
- ▶ Q. Chen, M.-C. Shiue, R.T. and J. Tribbia, Numerical approximation of the inviscid 3D primitive equations in a limited domain, to appear.

and a review article

- ▶ A. Rousseau, R.T., J. Tribbia in *Handbook of Numerical Analysis*, special volume on *Computational Methods for the Ocean and Atmosphere*, R. Temam and J. Tribbia, guest editors, P.G. Ciarlet Editor, Elsevier, 2009.

## Collaborations

- ▶ J. Tribbia (NCAR)
- ▶ Q. Chen, M.-C. Shiue and A. Rousseau

## Articles

- ▶ A. Rousseau, R.T., J. Tribbia, [RTT08], J. de Math. Pures et Appl., 2008.
- ▶ Q. Chen, M.-C. Shiue, and R.T., [CST09], The zero-mode of the inviscid Primitive Equations, J. Scient. Computing, to appear.
- ▶ Q. Chen, M.-C. Shiue, R.T. and J. Tribbia, Numerical approximation of the inviscid 3D primitive equations in a limited domain, to appear.

and a review article

- ▶ A. Rousseau, R.T., J. Tribbia in *Handbook of Numerical Analysis*, special volume on *Computational Methods for the Ocean and Atmosphere*, R. Temam and J. Tribbia, guest editors, P.G. Ciarlet Editor, Elsevier, 2009.

## Collaborations

- ▶ J. Tribbia (NCAR)
- ▶ Q. Chen, M.-C. Shiue and A. Rousseau

## Articles

- ▶ A. Rousseau, R.T., J. Tribbia, [RTT08], J. de Math. Pures et Appl., 2008.
- ▶ Q. Chen, M.-C. Shiue, and R.T., [CST09], The zero-mode of the inviscid Primitive Equations, J. Scient. Computing, to appear.
- ▶ Q. Chen, M.-C. Shiue, R.T. and J. Tribbia, Numerical approximation of the inviscid 3D primitive equations in a limited domain, to appear.

and a review article

- ▶ A. Rousseau, R.T., J. Tribbia in *Handbook of Numerical Analysis*, special volume on *Computational Methods for the Ocean and Atmosphere*, R. Temam and J. Tribbia, guest editors, P.G. Ciarlet Editor, Elsevier, 2009.

## Collaborations

- ▶ J. Tribbia (NCAR)
- ▶ Q. Chen, M.-C. Shiue and A. Rousseau

## Articles

- ▶ A. Rousseau, R.T., J. Tribbia, [RTT08], J. de Math. Pures et Appl., 2008.
- ▶ Q. Chen, M.-C. Shiue, and R.T., [CST09], The zero-mode of the inviscid Primitive Equations, J. Scient. Computing, to appear.
- ▶ Q. Chen, M.-C. Shiue, R.T. and J. Tribbia, Numerical approximation of the inviscid 3D primitive equations in a limited domain, to appear.

and a review article

- ▶ A. Rousseau, R.T., J. Tribbia in *Handbook of Numerical Analysis*, special volume on *Computational Methods for the Ocean and Atmosphere*, R. Temam and J. Tribbia, guest editors, P.G. Ciarlet Editor, Elsevier, 2009.

## SUMMARY

Whereas the PEs with viscosity resemble the incompressible Navier Stokes equations, up to a certain point, the nonviscous PEs, (also called hydrostatic Euler equations), do not resemble the incompressible Euler equations, as we will see below.

There are (at least) two major issues concerning these equations:

- ▶ A mathematical issue of well-posedness, and
- ▶ A computational/physical issue of appropriate boundary conditions for Limited Areas Models.

We will present some theoretical results concerning the linearized primitive equations and some computational results concerning the full nonlinear equations.

## SUMMARY

Whereas the PEs with viscosity resemble the incompressible Navier Stokes equations, up to a certain point, the nonviscous PEs, (also called hydrostatic Euler equations), do not resemble the incompressible Euler equations, as we will see below.

There are (at least) two major issues concerning these equations:

- ▶ A mathematical issue of well-posedness, and
- ▶ A computational/physical issue of appropriate boundary conditions for Limited Areas Models.

We will present some theoretical results concerning the linearized primitive equations and some computational results concerning the full nonlinear equations.

# 1. THE PRIMITIVE EQUATIONS OF THE OCEANS AND THE ATMOSPHERE

- The Primitive Equations (PEs) of the ocean and the atmosphere play a central role in a hierarchy of models aimed at describing the motion of the ocean and the atmosphere (General Circulation Models - GCM, Ocean General Circulation Models - OGCM). The PEs are directly derived from the fundamental laws of physics:
  - ▶ Equations of conservation of momentum, mass, and energy.
  - ▶ Equations for the salinity, equation of state.

# 1. THE PRIMITIVE EQUATIONS OF THE OCEANS AND THE ATMOSPHERE

- The Primitive Equations (PEs) of the ocean and the atmosphere play a central role in a hierarchy of models aimed at describing the motion of the ocean and the atmosphere (General Circulation Models - GCM, Ocean General Circulation Models - OGCM). The PEs are directly derived from the fundamental laws of physics:
  - ▶ Equations of conservation of momentum, mass, and energy.
  - ▶ Equations for the salinity, equation of state.

- **The unknowns:**

The velocity function  $\vec{V}_3 = \mathbf{v} + w\mathbf{e}_z$ , the temperature  $T$ , the pressure  $p$  and the density  $\rho$ . Possibly some other quantities such as the salinity (ocean) or the concentration of water (atmosphere)

- The PEs of the Ocean are obtained from the fundamental laws using the following assumptions:

- ▶ Boussinesq assumption,
- ▶ Hydrostatic assumption in the vertical direction.

- **The unknowns:**

The velocity function  $\vec{V}_3 = \mathbf{v} + w\mathbf{e}_z$ , the temperature  $T$ , the pressure  $p$  and the density  $\rho$ . Possibly some other quantities such as the salinity (ocean) or the concentration of water (atmosphere)

- The PEs of the Ocean are obtained from the fundamental laws using the following assumptions:
  - ▶ Boussinesq assumption,
  - ▶ Hydrostatic assumption in the vertical direction.

In Cartesian coordinates (in the so-called  $\beta$ -plane approximation) the Primitive Equation (PEs) without viscosity are as follows:

$$\left\{ \begin{array}{l} \frac{\partial \mathbf{v}}{\partial t} + (\mathbf{v} \cdot \nabla) \mathbf{v} + w \frac{\partial \mathbf{v}}{\partial z} + f \mathbf{k} \times \mathbf{v} + \nabla \phi = 0, \\ \frac{\partial \phi}{\partial z} = -\rho g, \\ \nabla \cdot \mathbf{v} + \frac{\partial w}{\partial z} = 0, \\ \frac{\partial T}{\partial t} + (\mathbf{v} \cdot \nabla) T + w \frac{\partial T}{\partial z} = 0, \quad \rho = \rho(T). \end{array} \right. \quad (1)$$

Whereas the theory of the PEs **with viscosity** resembles that of the incompressible Navier-Stokes, up to a certain point (that is before the recent works of Kobelkov, Cao and Titi, Kukavica and Ziane), the theory of PEs **without viscosity** does not resemble that of the Euler equations of incompressible fluids.

A fundamental mathematical difficulty concerning the PEs without viscosity is that *there is no set of local boundary conditions* for which these equations are well posed (Oliger and Sundstrom, 1978).

We now present this difficulty following Temam and Tribbia, *J. of Atm. Sciences*, 2003 [TeTr03].

## 2. ILL-POSEDNESS OF THE PRIMITIVE EQUATIONS

The PEs are linearized around a uniform stratified flow

$$\bar{u} = \bar{U}_0, \bar{v} = 0, \bar{T} = \bar{T}(z).$$

We set  $u' = u - \bar{u}$ , etc., dropping the primes we obtain the following equations for the disturbances:

$$\left\{ \begin{array}{l} u_t + \bar{U}_0 u_x - fv + \phi_x = 0, \\ v_t + \bar{U}_0 v_x + fu + \phi_y = 0, \\ T_t + \bar{U}_0 T_x + N^2 \frac{T_0}{g} w = 0, \\ u_x + v_y + w_z = 0, \\ \phi_z = \frac{gT}{T_0} (= \psi), \end{array} \right. \quad (2)$$

where

$$\bar{\rho} = \rho_0(1 - \alpha(\bar{T} - T_0)), \text{ and}$$

$$N^2 = -\frac{g}{\rho_0} \frac{d\bar{\rho}}{dz} = \text{the Brunt-Väisälä (buoyancy) frequency,}$$

assumed to be constant

## Modal Analysis

The domain is  $\mathcal{M} = \mathcal{M}' \times (-H, 0)$ , with  $\mathcal{M}' = (0, L_1) \times (0, L_2)$ ; and  $w = 0$  at  $z = 0, -H$ .

We first proceed by separation of variables and look for a solution of the form

$$u(x, y, z, t) = \mathcal{U}(z)u(x, y, t), \quad v(x, y, z, t) = \mathcal{V}(z)v(x, y, t), \quad \text{etc.}$$

Inserting these expressions in (2) we find by analysis that  $\mathcal{U}, \mathcal{V}, \mathcal{Z}, \Phi$  are proportional and we take them equal, and similarly  $\Psi$  and  $\mathcal{W}$  are (proportional) equal.

Furthermore  $\mathcal{U}$  and  $\mathcal{W} = \mathcal{U}'$  are solutions of a Sturm Liouville problem giving the solutions,  $\mathcal{U} = \mathcal{U}_n, \mathcal{W} = \mathcal{W}_n$  with

$$u_n = \sqrt{\frac{2}{H}} \cos(\lambda_n z), \quad w_n = \sqrt{\frac{2}{H}} \sin(\lambda_n z),$$

$$\lambda_n = \sqrt{\frac{1}{gH_n}} = \frac{n\pi}{H}, \quad n \geq 1, \text{ and}$$

$$u_0 = \sqrt{\frac{1}{H}}, \quad w_0 = 0, \quad \lambda_0 = 0.$$

We then look for a solution of (2) using the corresponding modal expansions, that is

$$\begin{aligned}
 u(x, y, z, t) &= \sum_n \mathcal{U}_n(z) u_n(x, y, t), \\
 v(x, y, z, t) &= \sum_n \mathcal{U}_n(z) v_n(x, y, t), \\
 T &= \sum_n \mathcal{U}_n(z) T_n(x, y, t) \\
 \phi(x, y, z, t) &= \sum_n \mathcal{U}_n(z) \phi_n(x, y, t), \\
 \psi &= \sum_n \mathcal{W}_n(z) \psi_n(x, y, t), \\
 w(x, y, z, t) &= \sum_n \mathcal{W}_n(z) w_n(x, y, t).
 \end{aligned} \tag{3}$$

We arrive, for each mode  $n$ , at the following system ( $\psi = \phi_z$ )

$$\left\{ \begin{aligned}
 u_{nt} + \bar{U}_0 u_{nx} - f v_n + \phi_{nx} &= 0, \\
 v_{nt} + \bar{U}_0 v_{nx} + f u_n + \phi_{ny} &= 0, \\
 \psi_{nt} + \bar{U}_0 \psi_{nx} + N^2 w_n &= 0, \\
 u_{nx} + v_{ny} + \lambda_n w_n &= 0 \\
 \psi_n &= -\lambda_n \phi_n.
 \end{aligned} \right. \tag{4}$$

The characteristic values of (4) are  $\bar{U}_0$ ,  $\bar{U}_0 + \lambda_n^{-1}$  and  $\bar{U}_0 - \lambda_n^{-1}$ . Counting characteristics, we see that if  $\lambda_n^{-1} < \bar{U}_0$  three boundary conditions are needed at  $x = 0$  (supercritical case), but if  $\lambda_n^{-1} > \bar{U}_0$ , two boundary conditions are needed at  $x = 0$  and one at  $x = L$  (subcritical case). Hence the global problem is ill-posed for any local set of boundary conditions.

The most challenging case is the subcritical case  $\lambda_n^{-1} > \bar{U}_0$ , which corresponds to just a few modes, *which are however the most energetic ones*.

For realistic values of the data ( $\bar{U}_0 \simeq 25m/s$ ,  $L \simeq$  a few thousands  $km$ ,  $H \simeq 10km$ ) there are about 5 subcritical modes, which are physically the most important and mathematically the most challenging.

Before we proceed we rewrite equation (4) in the form ( $n \geq 1$ ) :

$$\left\{ \begin{array}{l} \frac{\partial u_n}{\partial t} + \bar{U}_0 \frac{\partial u_n}{\partial x} - f v_n - \frac{1}{\lambda_n} \frac{\partial \psi_n}{\partial x} = 0; \\ \frac{\partial v_n}{\partial t} + \bar{U}_0 \frac{\partial v_n}{\partial x} + f u_n - \frac{1}{\lambda_n} \frac{\partial \psi_n}{\partial y} = 0, \\ \frac{\partial \psi_n}{\partial t} + \bar{U}_0 \frac{\partial \psi_n}{\partial x} - \frac{N^2}{\lambda_n} \left( \frac{\partial u_n}{\partial x} + \frac{\partial v_n}{\partial y} \right) = 0. \end{array} \right. \quad (5)$$

For  $n = 0$ ,  $w_0 = \psi_0 = 0$  and there remains

$$\left\{ \begin{array}{l} \frac{\partial u_0}{\partial t} + \bar{U}_0 \frac{\partial u_0}{\partial x} - f v_0 + \frac{\partial \phi_0}{\partial x} = 0, \\ \frac{\partial v_0}{\partial t} + \bar{U}_0 \frac{\partial v_0}{\partial x} + f u_0 + \frac{\partial \phi_0}{\partial y} = 0, \\ \frac{\partial u_0}{\partial x} + \frac{\partial v_0}{\partial y} = 0. \end{array} \right. \quad (6)$$

Note that, since the considered problem is linear, there is no coupling between the different modes; see the remark below about the nonlinear case which introduces these couplings.

Our aim is now to propose boundary conditions for (4)-(5) which make these equations well-posed and consequently Equations (2) also. The boundary conditions are different depending on whether

$$1 \leq n \leq n_c, \quad \text{or} \quad n > n_c,$$

where  $n_c, \lambda_{n_c}$  are such that

$$\frac{n_c \pi}{L_3} = \lambda_{n_c} < \frac{N}{\bar{U}_0} < \lambda_{n_c+1} = \frac{(n_c + 1)\pi}{L_3}. \quad (7)$$

We will not study the non generic case where  $L_3 N / \pi \bar{U}_0$  is an *integer*.

The modes  $0 \leq n \leq n_c$  are called *subcritical*, and the modes  $n > n_c$  are called *supercritical*.

### 3. STUDY OF THE EQUATIONS (5) - (6)

a) *The stationary equations associated with (5)-(6).*

The (physical) spatial domain under consideration will be  $\mathcal{M} = \mathcal{M}' \times (-H, 0)$ , where  $\mathcal{M}'$  is the interface atmosphere/ocean,  $\mathcal{M}' = (0, L_1) \times (0, L_2)$ .

We introduce, componentwise, the differential operators  $\mathcal{A}_n = (\mathcal{A}_{n1}, \mathcal{A}_{n2}, \mathcal{A}_{n3})$  operating on  $U_n = (u_n, v_n, \psi_n)$ ,

$$\mathcal{A}_n U_n = \begin{cases} \bar{U}_0 u_{nx} - \frac{1}{\lambda_n} \psi_{nx}, \\ \bar{U}_0 v_{nx} - \frac{1}{\lambda_n} \psi_{ny}, \\ \bar{U}_0 \psi_{nx} - \frac{N^2}{\lambda_n} (u_{nx} + v_{ny}), \end{cases} \quad (8)$$

with  $\bar{U}_0, N$  and  $\lambda_n > 0$  as above.

Our first remark concerns the nature of the stationary (time independent) equations in  $\mathcal{M}'$  :

$$\mathcal{A}_n U_n = F_n = (F_{un}, F_{vn}, F_{\psi n}), \quad n \geq 1. \quad (9)$$

Dropping the indices  $n$  we look for the characteristics of the differential system  $\mathcal{A}U = F$ ; that is in matrix form:

$$\mathcal{E}U_x + \mathcal{G}U_y = F. \quad (10)$$

After an easy calculation we find the real characteristic  $x = \text{const}$  for all modes and the two other characteristics are *imaginary for the subcritical modes* and *real for the supercritical ones*.

We infer from these remarks that the stationary system  $\mathcal{A}_n U_n = F_n$  is *fully elliptic* for the zero mode, *partly hyperbolic and partly elliptic* for the other subcritical modes (one real characteristic) and *fully hyperbolic* in the supercritical case (three real characteristics). This remark will be underlying the studies in Sections 4 and 5, although we do not use it directly.

*b) A trace theorem*

We consider the same differential operator  $\mathcal{A} = (\mathcal{A}_1, \mathcal{A}_2, \mathcal{A}_3)$ , as in (8) operating on  $U = (u, v, \psi)$ , but the indices  $n$  are dropped for the sake of simplicity:

$$\mathcal{A}U = (\bar{U}_0 u_x - \frac{1}{\lambda} \psi_x, \bar{U}_0 v_x - \frac{1}{\lambda} \psi_y, \bar{U}_0 \psi_x - \frac{N^2}{\lambda} (u_x + v_y))^T, \quad (11)$$

with  $\bar{U}_0, N, \lambda = \lambda_n > 0$  as above, and we consider the space.

$$\mathcal{X} = \left\{ U \in L^2(\mathcal{M}')^3, \mathcal{A}U \in L^2(\mathcal{M}')^3 \right\}, \quad (12)$$

endowed with its natural Hilbert norm

$$(|U|_{L^2(\mathcal{M}')^3}^2 + |\mathcal{A}U|_{L^2(\mathcal{M}')^3}^2)^{\frac{1}{2}}.$$

We have

**Theorem 3.1.** *If  $U = (u, v, \psi) \in \mathcal{X}$ , the traces of  $v$  and  $\psi$  are defined on all of  $\partial\mathcal{M}'$ , the trace of  $u$  is defined at  $x = 0$  and  $L_1$ , and they belong to the respective spaces  $H_x^{-1}(0, L_1)$  and  $H_y^{-1}(0, L_2)$ . Furthermore the trace operators are linear continuous in the corresponding spaces, e.g.  $U \in \mathcal{X} \rightarrow u|_{x=0}$  is continuous from  $\mathcal{X}$  into  $H_y^{-1}(0, L_2)$ .*

The proof is based on a repeated use of the idea of Lax and Phillips (1960).

#### 4. WELL POSEDNESS OF THE LINEARIZED EQUATION

Handled mode by mode and then globally for all modes.

**Subcritical Modes (One Subcritical Mode,  $1 \leq n \leq n_c$ )**

We temporarily drop the indices  $n$  and consider (5) when the mode is subcritical, that is  $\lambda = \lambda_n < N/\bar{U}_0$ .

We choose the following boundary conditions:

$$\begin{cases} \psi = 0 \text{ at } x = L_1, \text{ and } y = 0, L_2, \\ v = 0 \text{ and } u = \psi/\lambda\bar{U}_0 \text{ at } x = 0, \end{cases} \quad (13)$$

and we introduce the space

$$D(A) = \left\{ U \in L^2(\mathcal{M}')^3, \mathcal{A}U \in L^2(\mathcal{M}')^3, U \text{ satisfies (13)} \right\}, \quad (14)$$

and the operator<sup>1</sup>

$$AU = \mathcal{A}U, \quad \forall U \in D(A).$$

---

<sup>1</sup>When needed we will write also  $\mathcal{A}_n, A_n, D(A_n)$  to emphasize the dependence on  $n$  ( $\lambda = \lambda_n$ ).

a) *Regularity Result for  $D(A)$ .*

We now have a regularity result for  $U$  in  $D(A)$ .

**Theorem 4.1.** *If  $U = (u, v, \psi) \in D(A)$ , then  $v$  and  $\psi$  belong to  $H^1(\mathcal{M}')$  and  $u_x$  belongs to  $L^2(\mathcal{M}')$*

b) *Positivity of  $A$  and  $A^*$*

We endow the space  $H = L^2(\mathcal{M}')^3$  with the Hilbert scalar product and norm

$$(U, \tilde{U})_H = \int_{\Gamma_i} \left( u\tilde{u} + v\tilde{v} + \frac{1}{N^2}\psi\tilde{\psi} \right) d\mathcal{M}',$$
$$|U|_H = \{(U, U)_H\}^{1/2}.$$

To apply the Hille-Phillips-Yoshida theorem, we need to prove that  $A$  and its adjoint  $A^*$  are positive in the sense

$$\begin{cases} (AU, U)_H \geq 0, & \forall U \in D(A), \\ (A^*U, U)_H \geq 0, & \forall U \in D(A^*). \end{cases} \quad (15)$$

This result is proven by approximation using the regularity theorem.

$$\begin{aligned}
(AU, U)_H &= \int_{\Gamma_i} \left[ \bar{U}_0 u_x - \frac{1}{\lambda} \psi_x \right) u + \left( \left( \bar{U}_0 v_x - \frac{1}{\lambda} \psi_y \right) v \right. \\
&\quad \left. + \left( \frac{\bar{U}_0}{N^2} \psi_x - \frac{1}{\lambda} (u_x + v_y) \right) \psi \right] d\mathcal{M}' \\
&= \frac{\bar{U}_0}{2} \int_0^{L_2} (u^2 + v^2)(L_1, y) dy \\
&\quad - \int_0^{L_2} \left[ \frac{\bar{U}_0}{2} (u^2 + \frac{1}{N^2} \psi^2)(0, y) - \frac{1}{\lambda} (u\psi)(0, y) \right] dy \\
&\geq \frac{\bar{U}_0}{2} \int_0^{L_2} \left( (\lambda \bar{U}_0)^{-2} - N^{-2} \right) \psi^2(0, y) dy \geq 0.
\end{aligned}
\tag{16}$$

## Supercritical Modes

a) *The operator  $A$  and its adjoint  $A^*$*

Here, for one supercritical mode we choose the following boundary conditions:

$$\begin{cases} u, v, \text{ and } \psi = 0 \text{ at } x = 0, \\ \text{and } \psi = 0 \text{ at } y = 0 \text{ and } L_2. \end{cases} \quad (17)$$

In this case the operator  $A = A_n$ , is defined by  $AU = \mathcal{A}U$  as in (8), and

$$D(A) = \left\{ U \in H = L^2(\mathcal{M}')^2, \mathcal{A}U \in L^2(\mathcal{M}'), U \text{ satisfies (17)} \right\}. \quad (18)$$

We can then prove (5).

**Theorem 5.1.** *In the supercritical case, for every  $U \in D(A_n)$ ,  $A_n$  defined in (18), we have  $(A_n U, U)_{L^2(\mathcal{M}')^3} \geq 0$ . Similarly, we have  $(A_n^* U, U)_{L^2(\mathcal{M}')^3} \geq 0$ , for every  $U$  in  $D(A_n^*)$ ,  $A_n^*$  and  $D(A_n^*)$  appropriately defined.*

## **Subsequent steps**

The zeroth (barotropic) mode necessitates a whole analysis by itself.

Then we consider the whole system, and obtain again existence and uniqueness of solutions using the semigroup theory.

## 5. NUMERICAL IMPLEMENTATION FOR THE 3D-PEs

$$\left\{ \begin{array}{l} u_t + \bar{U}_0 u_x - fv + \phi_x = 0 \\ v_t + \bar{U}_0 v_x + f(\bar{U}_0 + u) + \phi_y = 0 \\ \psi_t + \bar{U}_0 \psi_x + N^2 w = 0 \\ \varphi_z = \psi \\ u_x + v_y + w_z = 0 \end{array} \right. \quad (19)$$

Normal modes expansion (in vertical direction)

$$\left\{ \begin{array}{l} (u, v, \phi) = \sum_{n \geq 0} \mathcal{U}_n(\mathbf{z})(u_n, v_n, \phi_n)(\mathbf{x}, y, t) \\ (w, \psi) = \sum_{n \geq 1} \mathcal{W}_n(\mathbf{z})(w_n, \psi_n)(\mathbf{x}, y, t) \end{array} \right. \quad (20)$$

The modes  $n \geq 1$

$$\begin{cases} u_{nt} + \bar{U}_0 u_{nx} - \frac{1}{N\lambda_n} \psi_{nx} - f v_n = 0, \\ v_{nt} + \bar{U}_0 v_{nx} + f u_n - \frac{1}{N\lambda_n} \psi_{ny} = 0, \\ \psi_{nt} + \bar{U}_0 \psi_{nx} - \frac{N}{\lambda_n} u_{nx} - \frac{N}{\lambda_n} v_{ny} = 0, \end{cases} \quad (21)$$

$$U_n = (u_n, v_n, \psi_n)^T$$

$$\frac{\partial U_n}{\partial t} + \mathbb{L}_n \frac{\partial U_n}{\partial x} + \mathbb{M}_n \frac{\partial U_n}{\partial y} + \mathbb{N}_n U_n = 0. \quad (22)$$

(51) is a symmetric hyperbolic system in two space variables

$$\mathbb{L}_n = \begin{pmatrix} \bar{U}_0 & 0 & -\frac{1}{\lambda_n} \\ 0 & \bar{U}_0 & 0 \\ -\frac{1}{\lambda_n} & 0 & \bar{U}_0 \end{pmatrix}, \quad \mathbb{M}_n = \begin{pmatrix} 0 & 0 & 0 \\ 0 & 0 & -\frac{1}{\lambda_n} \\ 0 & -\frac{1}{\lambda_n} & 0 \end{pmatrix}$$

$$\mathbb{N}_n = \begin{pmatrix} 0 & -f & 0 \\ f & 0 & 0 \\ 0 & 0 & 0 \end{pmatrix}$$

$\mathbb{L}_n$  has eigenvalues  $\bar{U}_0 + \frac{1}{\lambda_n}$ ,  $\bar{U}_0$  and  $\bar{U}_0 - \frac{1}{\lambda_n}$

$\mathbb{M}_n$  has eigenvalues  $0$ ,  $\frac{1}{\lambda_n}$ ,  $-\frac{1}{\lambda_n}$

Introduce  $\Sigma_n = (\xi_n, v_n, \eta_n)^T$

$$\begin{cases} \xi_n &= -\frac{\sqrt{2}}{2}u_n + \frac{\sqrt{2}}{2}\psi_n \\ v_n &= v_n \\ \eta_n &= \frac{\sqrt{2}}{2}u_n + \frac{\sqrt{2}}{2}\psi_n \end{cases}$$

$$\begin{cases} u_n &= -\frac{\sqrt{2}}{2}\xi_n + \frac{\sqrt{2}}{2}\eta_n \\ v_n &= v_n \\ \psi_n &= \frac{\sqrt{2}}{2}\xi_n + \frac{\sqrt{2}}{2}\eta_n \end{cases}$$

$$\{U_n = P\Sigma_n$$

$$\frac{\partial}{\partial t} \begin{pmatrix} \xi_n \\ v_n \\ \eta_n \end{pmatrix} + \begin{pmatrix} \bar{U}_0 + \frac{1}{\lambda_n} \\ \bar{U}_0 \\ \bar{U}_0 - \frac{1}{\lambda_n} \end{pmatrix} \frac{\partial}{\partial x} \begin{pmatrix} \xi_n \\ v_n \\ \psi_n \end{pmatrix} + \text{other terms} = 0.$$

## Boundary conditions

For  $1 \leq n \leq n_c$  (subcritical modes,  $\bar{U}_0 - \frac{1}{\lambda_n} < 0$ )

$$\left\{ \begin{array}{l} \xi_n(0, y, t) = 0 \\ v_n(0, y, t) = 0 \\ \eta_n(L_1, y, t) = 0. \end{array} \right. \quad (23)$$

For  $n > n_c$  (supercritical modes,  $\bar{U}_0 - \frac{1}{\lambda_n} > 0$ )

$$\left\{ \begin{array}{l} \xi_n(0, y, t) = 0 \\ v_n(0, y, t) = 0 \\ \eta_n(0, y, t) = 0 \end{array} \right. \quad (24)$$

Introduce also  $\Omega_n = (u_n, \alpha_n, \beta_n)^T$

$$\begin{cases} u_n = u_n \\ \alpha_n = \frac{\sqrt{2}}{2}v_n - \frac{\sqrt{2}}{2}\psi_n \\ \beta_n = \frac{\sqrt{2}}{2}v_n + \frac{\sqrt{2}}{2}\psi_n \end{cases} \quad \begin{cases} u_n = u_n \\ v_n = \frac{\sqrt{2}}{2}(\alpha_n + \beta_n) \\ \psi_n = -\frac{\sqrt{2}}{2}\alpha_n + \frac{\sqrt{2}}{2}\beta_n \end{cases} \quad (25)$$

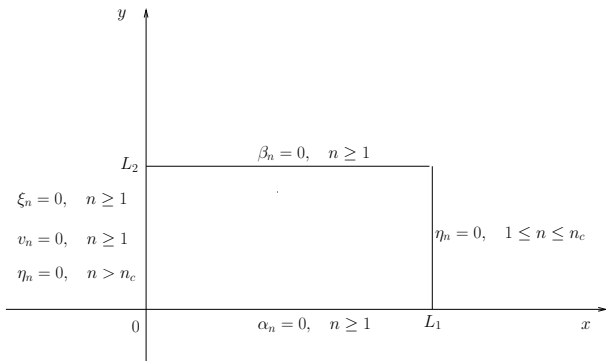
$$\{U_n = Q\Omega_n$$

$$\begin{cases} \frac{\partial}{\partial t} \begin{pmatrix} u_n \\ \alpha_n \\ \beta_n \end{pmatrix} + Q^{-1}L_nQ \frac{\partial}{\partial x} \begin{pmatrix} u_n \\ \alpha_n \\ \beta_n \end{pmatrix} + \\ \begin{pmatrix} 0 & & \\ & \frac{1}{\lambda_n} & \\ & & -\frac{1}{\lambda_n} \end{pmatrix} \frac{\partial}{\partial y} \begin{pmatrix} u_n \\ \alpha_n \\ \beta_n \end{pmatrix} + Q^{-1}N_nQ \begin{pmatrix} u_n \\ \alpha_n \\ \beta_n \end{pmatrix} = 0. \end{cases}$$

## Boundary Conditions

For all  $n \geq 1$

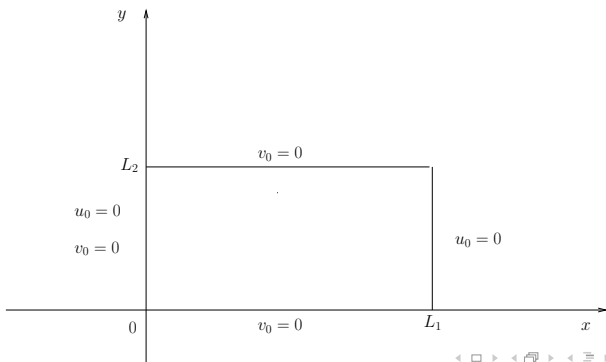
$$\left\{ \begin{array}{l} \alpha_n(x, 0, t) = 0 \\ \beta_n(x, L_2, t) = 0 \end{array} \right. \quad (26)$$



## The zeroth mode

$$\begin{cases} u_{0t} + \bar{U}_0 u_{0x} + \phi_{0x} - f v_0 = 0, \\ v_{0t} + \bar{U}_0 v_{0x} + \phi_{0y} + f u_0 + F_0 = 0, F_0 = \sqrt{L_3} f \bar{U}_0, \\ u_{0x} + v_{0y} = 0. \end{cases} \quad (27)$$

## Euler type equations



## Numerical scheme for the zero mode

Let  $\Delta t = T/K$ ,  $\mathbf{v}^k \approx \mathbf{v}(x, y, k\Delta t)$ , and  $\mathbf{v}^{k+\frac{1}{2}}$  represents an intermediate value between  $\mathbf{v}^k$  and  $\mathbf{v}^{k+1}$ , etc.

First Step:

$$\begin{cases} \frac{\mathbf{v}^{k+\frac{1}{2}} - \mathbf{v}^k}{\Delta t} + \bar{U}_0 \mathbf{v}_x^{k+\frac{1}{2}} + f\mathbf{k} \times \mathbf{v}^k + \nabla \phi_0^k + \mathbf{G}_0^k = 0, \\ \mathbf{v}^{k+\frac{1}{2}}|_{x=0} = 0, \end{cases} \quad (28)$$

Here

$$\mathbf{G}_0^k = \begin{pmatrix} \int_{-L_3}^0 B(u^k, v^k, w^k; u^k) \mathcal{U}_0(z) dz \\ \int_{-L_3}^0 B(u^k, v^k, w^k; v^k) \mathcal{U}_0(z) dz + f\bar{U}_0\sqrt{H} \end{pmatrix}, \quad (29)$$

Second Step: (projection method)

$$\begin{cases} \frac{\mathbf{v}^{k+1} - \mathbf{v}^{k+\frac{1}{2}}}{\Delta t} + \nabla(\phi_0^{k+1} - \phi_0^k) = 0, \\ \nabla \cdot \mathbf{v}^{k+1} = 0, \\ \mathbf{v}^{k+1} \cdot \mathbf{n} = 0 \text{ on } \partial\mathcal{M}'. \end{cases} \quad (30)$$

## Neumann Problem

From the Second Step, we can find  $\phi_0^{k+1}$  by solving the Neumann problem

$$\begin{cases} \Delta \phi_0^{k+1} = \Delta \phi_0^k + \frac{\nabla \cdot \mathbf{v}^{k+\frac{1}{2}}}{\Delta t}, \\ \nabla \phi_0^{k+1} \cdot \mathbf{n} = \frac{\mathbf{v}^{k+\frac{1}{2}}}{\Delta t}, \quad \partial \mathcal{M}'. \end{cases} \quad (31)$$

and imposing the compatibility condition

$$\int_{\mathcal{M}'} \phi_0^{k+1} dx dy = 0.$$

## Stability Issue

Given the mesh size  $\mathbf{h} = (\Delta x, \Delta y)$ , we have the following stability result:

### Lemma 1

*If  $\Delta t$  and  $S(\mathbf{h})$  satisfy the conditions*

$$\Delta t S^4(\mathbf{h}) \leq \frac{1}{c_1^2 K_4}, \quad \Delta t \leq \frac{1}{8}, \quad \text{where } S^2(\mathbf{h}) = \frac{1}{(\Delta x)^2} + \frac{1}{(\Delta y)^2}, \quad (32)$$

*then, for  $0 \leq n \leq N_T$ , we have*

$$|\mathbf{v}_{\mathbf{h}}^n|_{\mathbf{h}}^2 \leq K_4, \quad (\Delta t)^3 \sum_{k=1}^{N_T} |\nabla_{\mathbf{h}} \phi_{\mathbf{h}}^k|_{\mathbf{h}}^2 \leq K_4. \quad (33)$$

## The subcritical and supercritical modes

We rewrite (6) in the matrix form as follows:

$$\frac{\partial U_n}{\partial t} + E_n \frac{\partial U_n}{\partial x} + F_n \frac{\partial U_n}{\partial y} + G_n = 0. \quad (34)$$

Here,

$$U_n = \begin{pmatrix} u_n \\ v_n \\ \psi_n \end{pmatrix}, E_n = \begin{pmatrix} \bar{U}_0 & 0 & \frac{-1}{\lambda_n} \\ 0 & \bar{U}_0 & 0 \\ \frac{-N^2}{\lambda_n} & 0 & \bar{U}_0 \end{pmatrix}, F_n = \begin{pmatrix} 0 & 0 & 0 \\ 0 & 0 & \frac{-1}{\lambda_n} \\ 0 & \frac{-N^2}{\lambda_n} & 0 \end{pmatrix} \quad (35)$$

and

$$G_n = \begin{pmatrix} -fv_n + \int_{-H}^0 B(u, v, w; u) \mathcal{U}_n(z) dz \\ fu_n + \int_{-H}^0 B(u, v, w; v) \mathcal{U}_n(z) dz \\ \int_{-H}^0 B(u, v, w; \psi) \mathcal{W}_n(z) dz \end{pmatrix}. \quad (36)$$

## Change of Variables

Change of variables:

$$\begin{pmatrix} \xi_n \\ v_n \\ \eta_n \end{pmatrix} = \begin{pmatrix} u_n - \frac{\psi_n}{N} \\ v_n \\ u_n + \frac{\psi_n}{N} \end{pmatrix}, \quad \begin{pmatrix} u_n \\ \alpha_n \\ \beta_n \end{pmatrix} = \begin{pmatrix} u_n \\ v_n + \frac{\psi_n}{N} \\ v_n - \frac{\psi_n}{N} \end{pmatrix}. \quad (37)$$

## Boundary Conditions for the subcritical modes

Boundary conditions for the subcritical modes:

$$\left\{ \begin{array}{l} \xi_n(0, y, t) = 0, \\ v_n(0, y, t) = 0, \\ \eta_n(L_1, y, t) = 0. \end{array} \right. \quad \left\{ \begin{array}{l} \alpha_n(x, L_2, t) = 0, \\ \beta_n(x, 0, t) = 0. \end{array} \right. \quad (38)$$

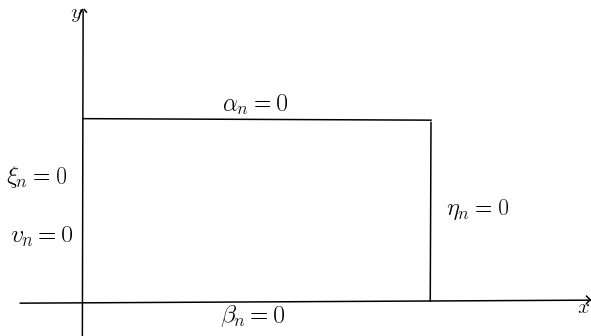


**FIGURE 1:** *Boundary conditions for the subcritical modes*

## Boundary conditions for the supercritical modes

Boundary conditions for the supercritical modes:

$$\left\{ \begin{array}{l} \xi_n(0, y, t) = 0, \\ v_n(0, y, t) = 0, \\ \eta_n(0, y, t) = 0. \end{array} \right. \quad \left\{ \begin{array}{l} \alpha_n(x, L_2, t) = 0, \\ \beta_n(x, 0, t) = 0. \end{array} \right. \quad (39)$$

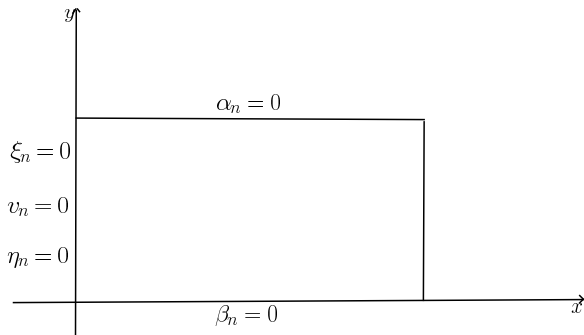


**FIGURE 2:** *Boundary conditions for the supercritical modes*

## Numerical Schemes for the subcritical modes

Splitting method:

The First Step:

$$\frac{U_n^{k+\frac{1}{2}} - U_n^k}{\Delta t} + E_n \frac{\partial U_n^{k+\frac{1}{2}}}{\partial x} + G_n^k = 0. \quad (40)$$

The Second Step:

$$\frac{U_n^{k+1} - U_n^{k+\frac{1}{2}}}{\Delta t} + F_n \frac{\partial U_n^{k+1}}{\partial y} = 0. \quad (41)$$

### Remark

- ▶ *This is a partly implicit scheme.*

## Numerical scheme for the subcritical modes

The First Step:

$$\left\{ \begin{array}{l} \frac{\xi_{n,i,j}^{k+\frac{1}{2}} - \xi_{n,i,j}^k}{\Delta t} + (\bar{U}_0 + \frac{N}{\lambda_n}) \frac{\xi_{n,i,j}^{k+\frac{1}{2}} - \xi_{n,i-1,j}^{k+\frac{1}{2}}}{\Delta x} = S_{n,i,j}^{k,1}, i = 2, \dots, l+1, \\ \frac{v_{n,i,j}^{k+\frac{1}{2}} - v_{n,i,j}^k}{\Delta t} + \bar{U}_0 \frac{v_{n,i,j}^{k+\frac{1}{2}} - v_{n,i-1,j}^{k+\frac{1}{2}}}{\Delta x} = S_{n,i,j}^{k,2}, i = 2, \dots, l+1, \\ \frac{\eta_{n,i,j}^{k+\frac{1}{2}} - \eta_{n,i,j}^k}{\Delta t} + (\bar{U}_0 - \frac{N}{\lambda_n}) \frac{\eta_{n,i+1,j}^{k+\frac{1}{2}} - \eta_{n,i,j}^{k+\frac{1}{2}}}{\Delta x} = S_{n,i,j}^{k,3}, i = 1, \dots, l, \\ \text{and } j = 1, \dots, J+1 \text{ in all cases,} \end{array} \right. \quad (42)$$

where

$S_{n,i,j}^{k,1}$ ,  $S_{n,i,j}^{k,2}$  and  $S_{n,i,j}^{k,3}$  are nonlinear terms.

## Numerical scheme for the subcritical modes

The boundary conditions for  $\xi_n^{k+\frac{1}{2}}$ ,  $v_n^{k+\frac{1}{2}}$  and  $\eta_n^{k+\frac{1}{2}}$  are

$$\xi_{n,0,j}^{k+\frac{1}{2}} = 0, \quad v_{n,0,j}^{k+\frac{1}{2}} = 0, \quad \eta_{n,l,j}^{k+\frac{1}{2}} = 0, \quad \text{for } 0 \leq j \leq J, \quad (43)$$

The Second Step

$$\left\{ \begin{array}{l} \frac{u_{n,i,j}^{k+1} - u_{n,i,j}^{k+\frac{1}{2}}}{\Delta t} = 0, \\ \frac{\alpha_{n,i,j}^{k+1} - \alpha_{n,i,j}^{k+\frac{1}{2}}}{\Delta t} - \frac{N}{\lambda_n} \frac{\alpha_{n,i,j+1}^{k+1} - \alpha_{n,i,j}^{k+1}}{\Delta y} = 0, \\ \frac{\beta_{n,i,j}^{k+1} - \beta_{n,i,j}^{k+\frac{1}{2}}}{\Delta t} + \frac{N}{\lambda_n} \frac{\beta_{n,i,j}^{k+1} - \beta_{n,i,j-1}^{k+1}}{\Delta y} = 0 \end{array} \right. \quad (44)$$

The boundary conditions for  $\alpha_n^{k+1}$ ,  $\beta_n^{k+1}$  are

$$\left\{ \begin{array}{l} \alpha_{n,l,j}^{k+1} = 0, \quad \text{for } 0 \leq j \leq J, \\ \beta_{n,i,0}^{k+1} = 0, \quad \text{for } 0 \leq i \leq l. \end{array} \right. \quad (45)$$

## Numerical schemes for the supercritical modes

Splitting method:

The First Step:

$$\left\{ \begin{array}{l} \frac{\xi_{n,i,j}^{k+\frac{1}{2}} - \xi_{n,i,j}^k}{\Delta t} + (\bar{U}_0 + \frac{N}{\lambda_n}) \frac{\xi_{n,i,j}^{k+\frac{1}{2}} - \xi_{n,i-1,j}^{k+\frac{1}{2}}}{\Delta x} = S_{n,i,j}^{k,1}, i = 2, \dots, l+1, \\ \frac{v_{n,i,j}^{k+\frac{1}{2}} - v_{n,i,j}^k}{\Delta t} + \bar{U}_0 \frac{v_{n,i,j}^{k+\frac{1}{2}} - v_{n,i-1,j}^{k+\frac{1}{2}}}{\Delta x} = S_{n,i,j}^{k,2}, i = 2, \dots, l+1, \\ \frac{\eta_{n,i,j}^{k+\frac{1}{2}} - \eta_{n,i,j}^k}{\Delta t} + (\bar{U}_0 - \frac{N}{\lambda_n}) \frac{\eta_{n,i,j}^{k+\frac{1}{2}} - \eta_{n,i-1,j}^{k+\frac{1}{2}}}{\Delta x} = S_{n,i,j}^{k,3}, i = 1, \dots, l, \\ \text{and } i = 1, \dots, J+1 \text{ in all cases,} \end{array} \right. \quad (46)$$

The boundary conditions for  $\xi_n^{k+\frac{1}{2}}$ ,  $v_n^{k+\frac{1}{2}}$  and  $\eta_n^{k+\frac{1}{2}}$  are, for  $0 \leq j \leq J$ ,

$$\xi_{n,0,j}^{k+\frac{1}{2}} = 0, \quad v_{n,0,j}^{k+\frac{1}{2}} = 0, \quad \eta_{n,0,j}^{k+\frac{1}{2}} = 0. \quad (47)$$

## Numerical schemes for the supercritical modes

The second Step:

$$\left\{ \begin{array}{l} \frac{u_{n,i,j}^{k+1} - u_{n,i,j}^{k+\frac{1}{2}}}{\Delta t} = 0, \\ \frac{\alpha_{n,i,j}^{k+1} - \alpha_{n,i,j}^{k+\frac{1}{2}}}{\Delta t} - \frac{N}{\lambda_n} \frac{\alpha_{n,i,j+1}^{k+1} - \alpha_{n,i,j}^{k+1}}{\Delta y} = 0, \\ \frac{\beta_{n,i,j}^{k+1} - \beta_{n,i,j}^{k+\frac{1}{2}}}{\Delta t} + \frac{N}{\lambda_n} \frac{\beta_{n,i,j}^{k+1} - \beta_{n,i,j-1}^{k+1}}{\Delta y} = 0 \end{array} \right. \quad (48)$$

The boundary conditions for  $\alpha_n^{k+1}$ ,  $\beta_n^{k+1}$  are

$$\left\{ \begin{array}{ll} \alpha_{n,l,j}^{k+1} = 0, & \text{for } 0 \leq j \leq J, \\ \beta_{n,i,0}^{k+1} = 0, & \text{for } 0 \leq i \leq I. \end{array} \right. \quad (49)$$

## Treatment of the integral of the nonlinear term

In our study, we only need to consider a small number of modes ( $\leq 10$ ), and it is then appropriate to transform these integrals into the sums of the Fourier coefficients.

## Numerical Simulations in a nested domain

Consider two domains as follows:

The larger domain:

$$\mathcal{M} = (0, L_1) \times (0, L_2) \times (-L_3, 0)$$

The middle-half domain:

$$\mathcal{M}_1 = (L_1/4, 3L_1/4) \times (L_2/4, 3L_2/4) \times (-L_3, 0)$$

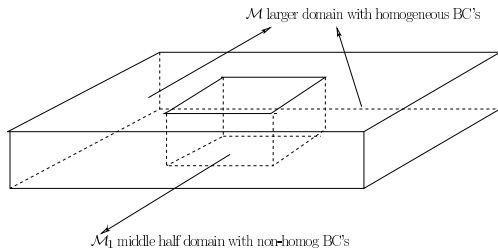


**FIGURE 3:** The larger domain  $\mathcal{M}$  and the middle half domain  $\mathcal{M}_1$ .

## Numerical simulations in a nested domain

### Objectives:

- ▶ Given the initial and boundary conditions, we perform simulations on the larger domain.
- ▶ We perform simulations on the middle-half domain using the initial and boundary conditions provided from Step 1.
- ▶ We consider the data from Step 1 as the true solution, and compare these two data from Step 1 and Step 2 in the middle-half domain and compute relative errors.

## Numerical simulations in a nested domain

### Objectives:

- ▶ Given the initial and boundary conditions, we perform simulations on the larger domain.
- ▶ We perform simulations on the middle-half domain using the initial and boundary conditions provided from Step 1.
- ▶ We consider the data from Step 1 as the true solution, and compare these two data from Step 1 and Step 2 in the middle-half domain and compute relative errors.

## Numerical simulations in a nested domain

### Objectives:

- ▶ Given the initial and boundary conditions, we perform simulations on the larger domain.
- ▶ We perform simulations on the middle-half domain using the initial and boundary conditions provided from Step 1.
- ▶ We consider the data from Step 1 as the true solution, and compare these two data from Step 1 and Step 2 in the middle-half domain and compute relative errors.

## Numerical Experiments

In the simulation, the initial conditions are given by these scalar functions:

$$\left\{ \begin{array}{l} u(x, y, z, 0) = \frac{x}{L_1} \frac{2\pi}{L_2} \sin\left(\frac{2\pi x}{L_1}\right) \cos\left(\frac{2\pi y}{L_2}\right) + \sin\left(\frac{4\pi x}{L_1}\right) \cos\left(\frac{4\pi y}{L_2}\right) \\ \quad \cos\left(\frac{\pi z}{H}\right), \\ v(x, y, z, 0) = \frac{-1}{L_1} \left( \sin\left(\frac{2\pi x}{L_1}\right) + \frac{2\pi x}{L_1} \cos\left(\frac{2\pi x}{L_1}\right) \right) \sin\left(\frac{2\pi y}{L_2}\right) \\ \quad + \frac{L_2}{L_1} \left( \sin^2\left(\frac{4\pi x}{L_1}\right) + \sin\left(\frac{4\pi x}{L_1}\right) \sin\left(\frac{4\pi y}{L_2}\right) \cos\left(\frac{\pi z}{H}\right) \right), \\ w(x, y, z, 0) = \frac{-4H}{L_1} \left( \sin\left(\frac{4\pi x}{L_1}\right) + \cos\left(\frac{4\pi x}{L_1}\right) \right) \cos\left(\frac{4\pi y}{L_2}\right) \sin\left(\frac{\pi z}{H}\right), \\ \phi(x, y, z, 0) = \bar{U}_0 \sin\left(\frac{2\pi x}{L_1}\right) \sin\left(\frac{2\pi y}{L_2}\right) \left( \cos\left(\frac{\pi z}{H}\right) - \cos\left(\frac{2\pi z}{H}\right) \right), \\ \psi(x, y, z, 0) = \frac{\pi \bar{U}_0}{H} \sin\left(\frac{2\pi x}{L_1}\right) \sin\left(\frac{2\pi y}{L_2}\right) \left( 2 \sin\left(\frac{2\pi z}{H}\right) - \sin\left(\frac{\pi z}{H}\right) \right). \end{array} \right. \quad (50)$$

## Numerical Experiments

Boundary conditions: homogeneous conditions for the *zero mode*,

$$\begin{cases} u_0(0, y, t) = 0, & u_0(L_1, y, t) = 0, \\ v_0(0, y, t) = 0, & v_0(x, 0, t) = 0, & v_0(x, L_2, t) = 0; \end{cases} \quad (51)$$

for the *subcritical modes*, i.e. when  $1 \leq n < n_c$ ,

$$\begin{cases} \xi_n(0, y, t) = 0, & v_n(0, y, t) = 0, & \eta_n(L_1, y, t) = 0, \\ \alpha_n(x, L_2, t) = 0, & \beta_n(x, 0, t) = 0; \end{cases} \quad (52)$$

and for the *supercritical modes*, i.e. when  $n > n_c$ ,

$$\begin{cases} \xi_n(0, y, t) = 0, & v_n(0, y, t) = 0, & \eta_n(0, y, t) = 0, \\ \alpha_n(x, L_2, t) = 0, & \beta_n(x, 0, t) = 0. \end{cases} \quad (53)$$

## Numerical Experiments

The physical parameters:

The length of the domain in $x$ – direction	$L_1 = 10^3$ km,
The length of the domain in $y$ – direction	$L_2 = 500$ km,
The length of the domain in $z$ – direction	$L_3 = 10$ km ,
The constant reference velocity	$\bar{U}_0 = 20$ m/s,
The Coriolis parameter	$f = 10^{-4}$ ,
The Brunt–Väisälä (buoyancy) frequency	$N = 10^{-2}$ ,
The final time	$T = 5 \times 10^4$ s ,
The number of modes	$N_{max} = 5$ .

## Numerical Experiments

The numerical parameters:

- The number of time steps  $N_T = 1600$ ,
- The number of mesh grids in  $x$   $N_x = 400$ ,
- The number of mesh grids in  $y$   $N_y = 200$ ,
- The number of mesh grids in  $z$   $N_z = 40$ .

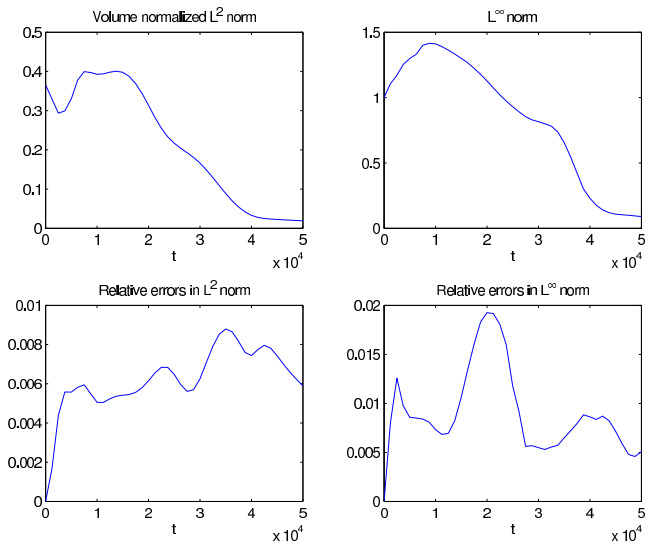


**FIGURE 4:** Top row: evolution of the solution  $u$  in the  $L^2$  and  $L^\infty$  norms. Bottom row: evolution of the relative errors for  $u$  in the  $L^2$  and  $L^\infty$  norms.

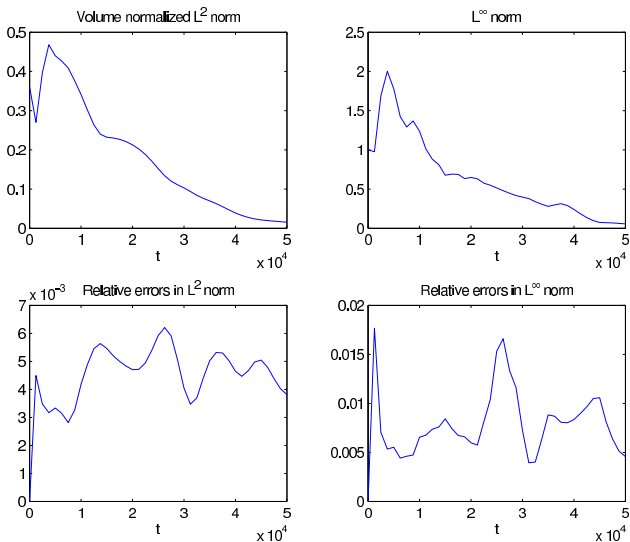


**FIGURE 5:** Top row: evolution of the solution  $v$  in the  $L^2$  and  $L^\infty$  norms. Bottom row: evolution of the relative errors for  $v$  in the  $L^2$  and  $L^\infty$  norms.

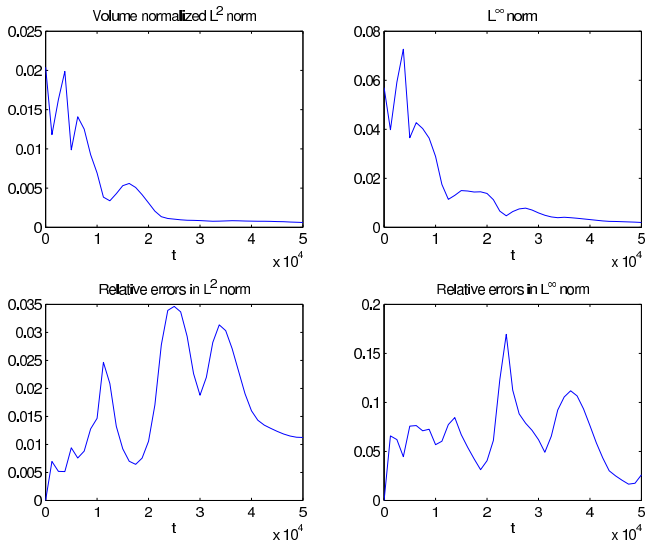


**FIGURE 6:** Top row: evolution of the solution  $w$  in the  $L^2$  and  $L^\infty$  norms. Bottom row: evolution of the relative errors for  $w$  in the  $L^2$  and  $L^\infty$  norms.

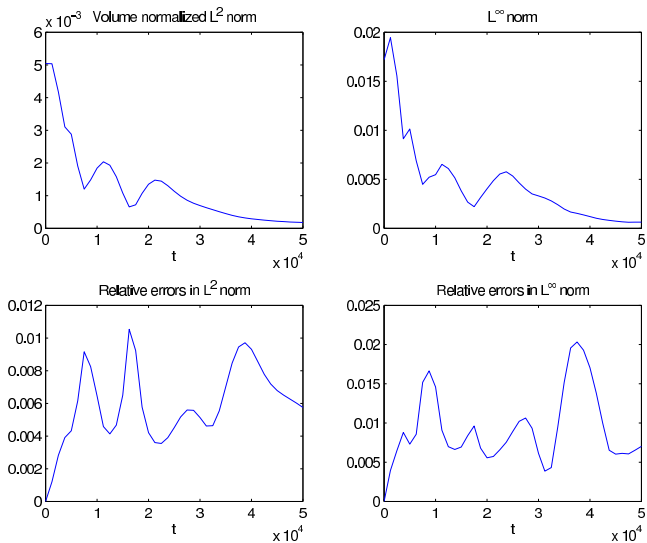


**FIGURE 7:** Top row: evolution of the solution  $\psi$  in the  $L^2$  and  $L^\infty$  norms. Bottom row: evolution of the relative errors for  $\psi$  in the  $L^2$  and  $L^\infty$  norms.

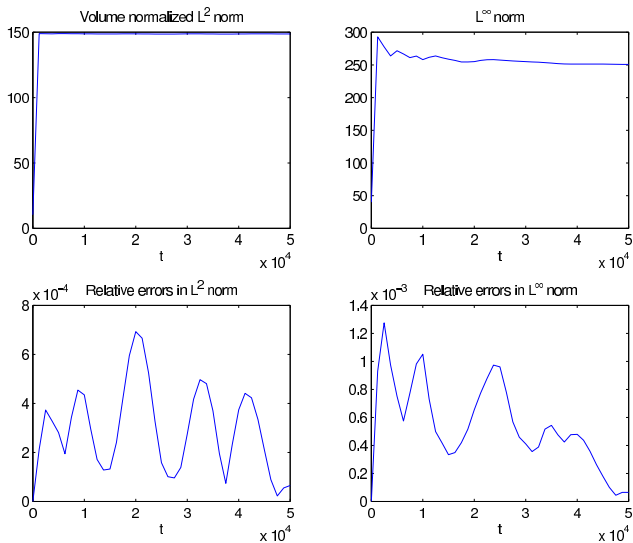


**FIGURE 8:** Top row: evolution of the solution  $\phi$  in  $L^2$  and  $L^\infty$  norms. Bottom row: evolution of the relative errors for  $\phi$  in  $L^2$  and  $L^\infty$  norms.

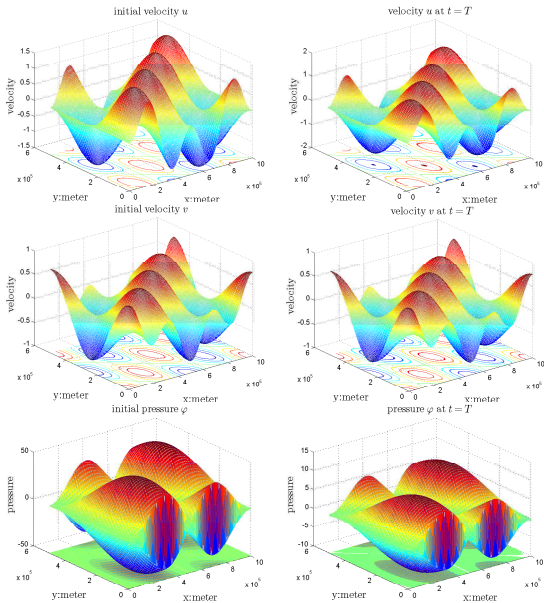


**FIGURE 9:** *The exact velocity  $u$ ,  $v$  and pressure  $\varphi$  at  $t = 0$  (on the left); the approximated velocity  $u$ ,  $v$  and pressure  $\varphi$  at  $t = T$  (on the right).*

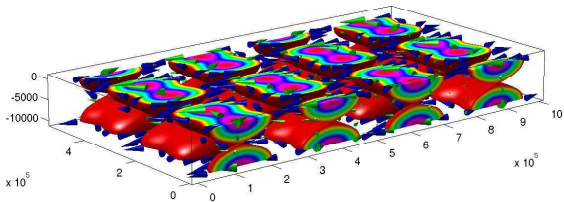


**FIGURE 10:** *The initial state of velocity field in the larger domain  $\mathcal{M}$*

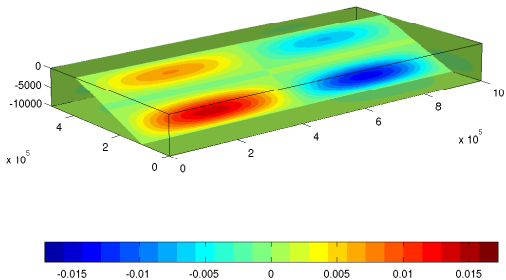


**FIGURE 11:** *The initial state of  $\psi$  in the larger domain  $\mathcal{M}$*

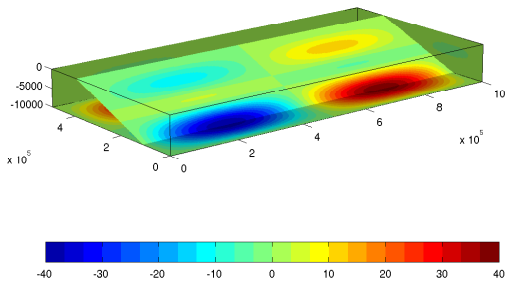


**FIGURE 12:** *The initial state of  $\phi$  in the larger domain  $\mathcal{M}$*

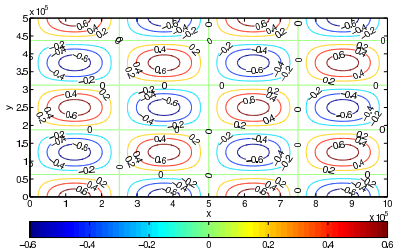


FIGURE 13: Contour plot of  $u$  at  $z = -2500\text{m}$ , at  $t = 0$ .

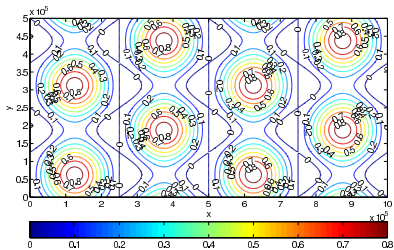


FIGURE 14: Contour plot of  $v$  at  $z = -2500\text{m}$ , at  $t = 0$ .

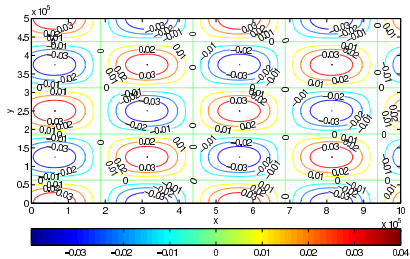


FIGURE 15: Contour plot of  $w$  at  $z = -2500\text{m}$ , at  $t = 0$ .

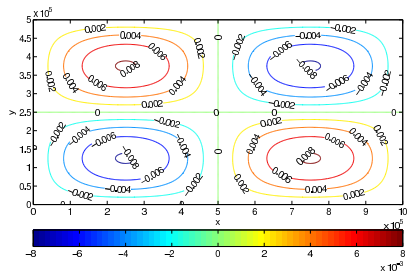
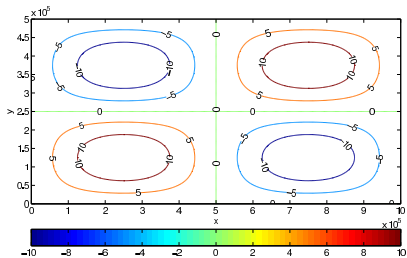
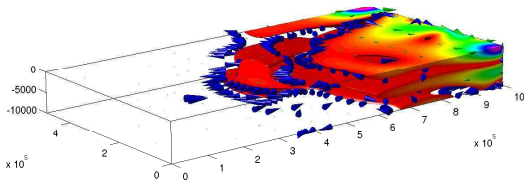


FIGURE 16: Contour plot of  $\psi$  at  $z = -2500\text{m}$ , at  $t = 0$ .



**FIGURE 17:** Contour plot of  $\phi$  at  $z = -2500\text{m}$ , at  $t = 0$ .



**FIGURE 18:** The velocity field with cone plot in the larger domain  $\mathcal{M}$  at  $t = T$

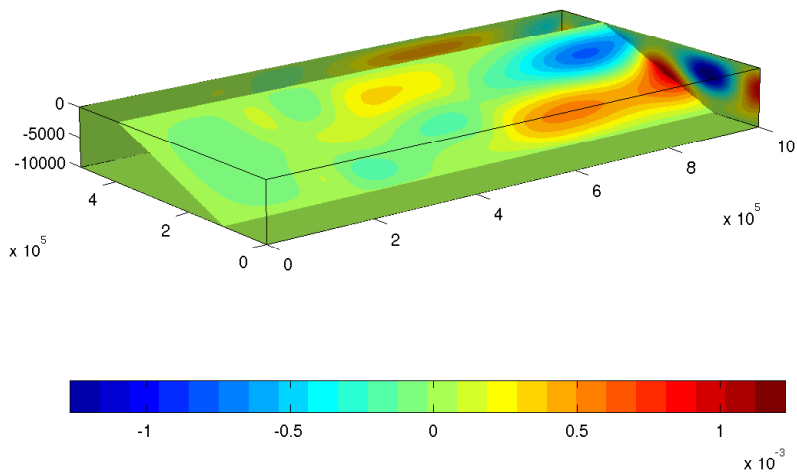


**FIGURE 19:** *The state of  $\psi$  in the larger domain  $\mathcal{M}$  at  $t = T$ .*

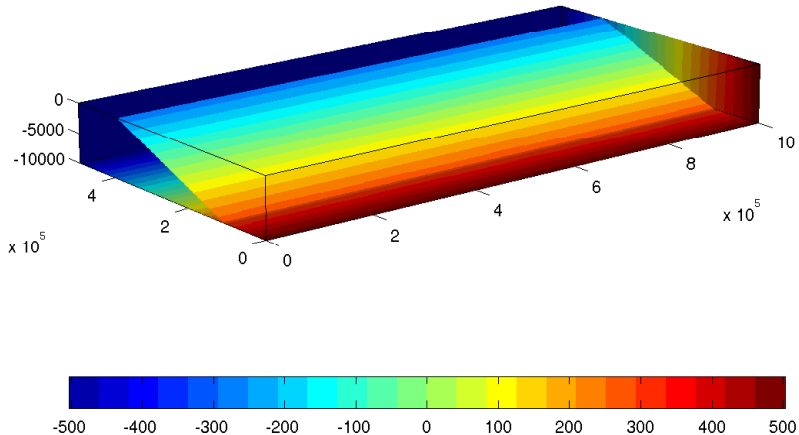


**FIGURE 20:** *The state of  $\phi$  in the larger domain  $\mathcal{M}$  at  $t = T$ .*

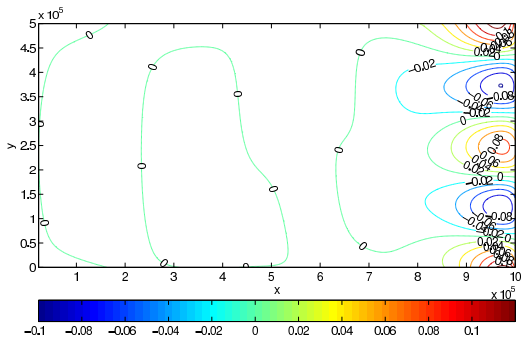


**FIGURE 21:** Contour plot of  $u$  at  $z = -2500\text{m}$ , at  $t = T$ .

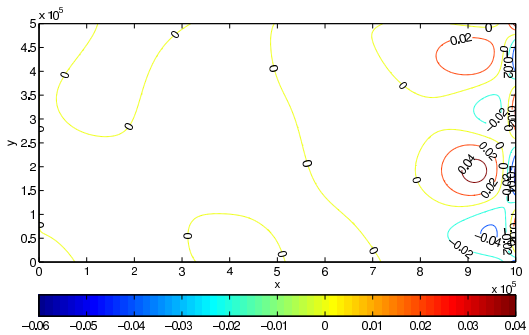


**FIGURE 22:** Contour plot of  $v$  at  $z = -2500\text{m}$ , at  $t = T$ .

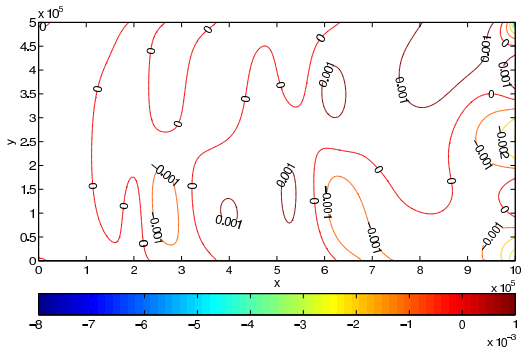


**FIGURE 23:** Contour plot of  $w$  at  $z = -2500\text{m}$ , at  $t = T$ .

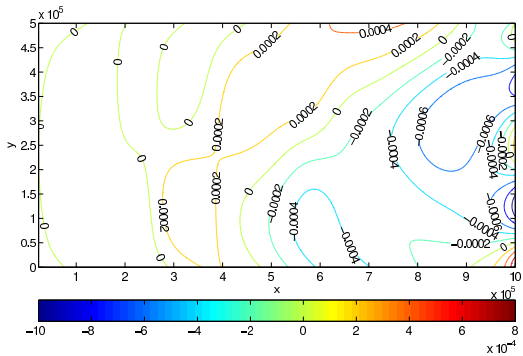


**FIGURE 24:** Contour plot of  $\psi$  at  $z = -2500\text{m}$ , at  $t = T$ .

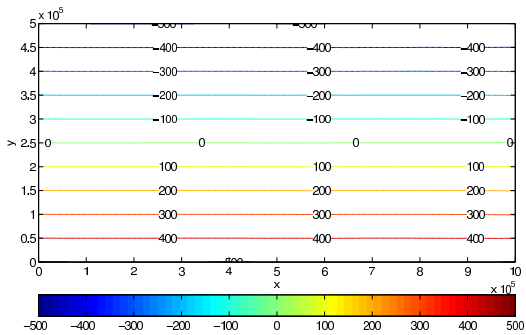


**FIGURE 25:** Contour plot of  $\phi$  at  $z = -2500m$ , at  $t = T$ .

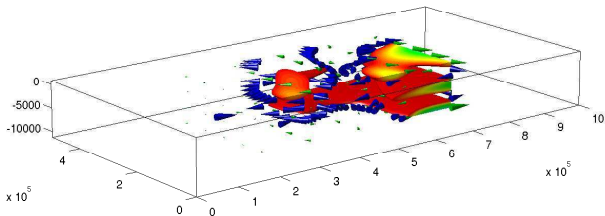


**FIGURE 26:** *The velocity field with cone plot in the middle half domain  $\mathcal{M}_1$  at  $t = T$*

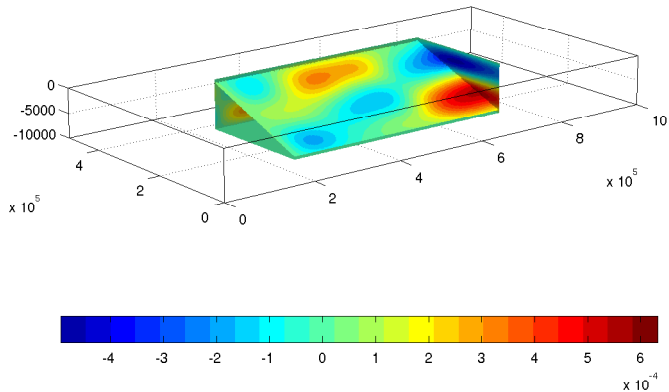


**FIGURE 27:** *The state of  $\psi$  in the middle half domain  $\mathcal{M}_1$  at  $t = T$ .*

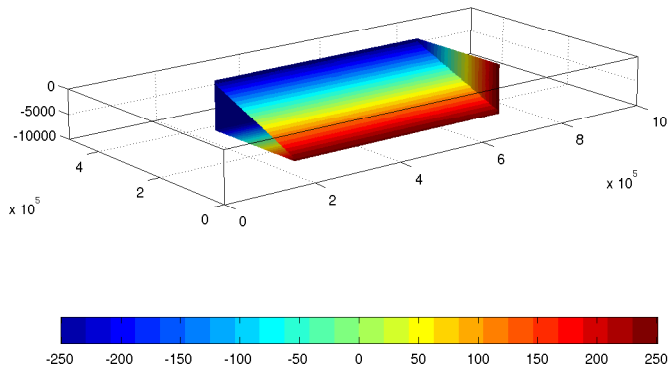


**FIGURE 28:** *The state of  $\phi$  in the middle half domain  $\mathcal{M}_1$  at  $t = T$ .*

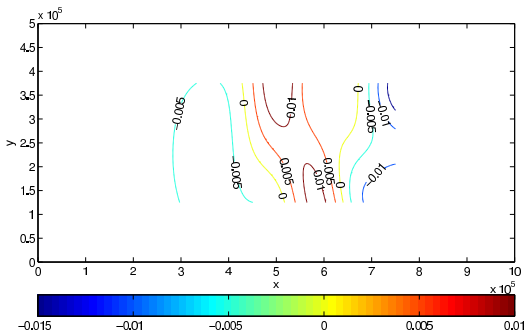


**FIGURE 29:** Contour plot of  $u$  at  $z = -2500\text{m}$ , at  $t = T$ .

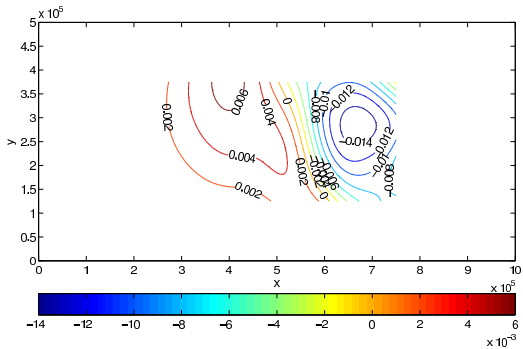


**FIGURE 30:** Contour plot of  $v$  at  $z = -2500\text{m}$ , at  $t = T$ .

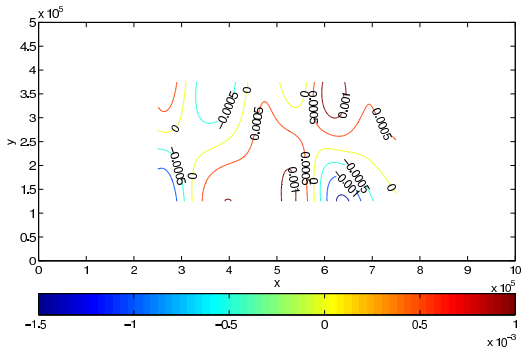


**FIGURE 31:** Contour plot of  $w$  at  $z = -2500\text{m}$ , at  $t = T$ .

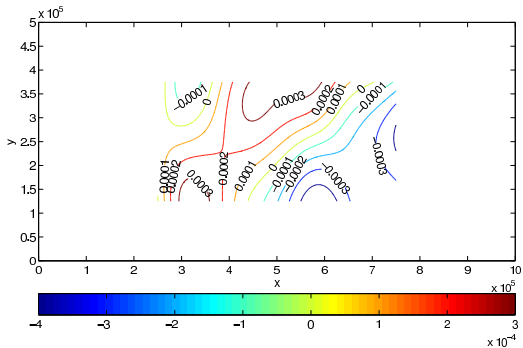


**FIGURE 32:** Contour plot of  $\psi$  at  $z = -2500\text{m}$ , at  $t = T$ .

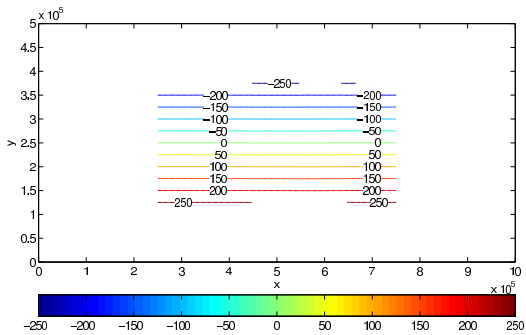


**FIGURE 33:** Contour plot of  $\phi$  at  $z = -2500m$ , at  $t = T$ .

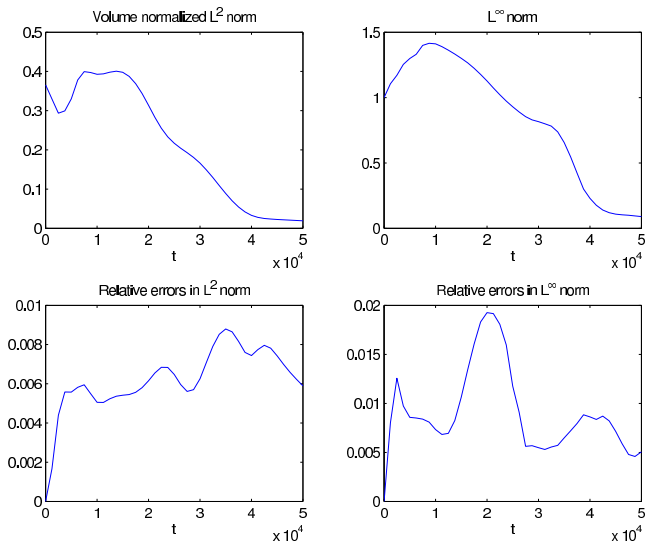


**FIGURE 34:** Top row: evolution of the solution  $u$  in  $L^2$  and  $L^\infty$  norms. Bottom row: evolution of the relative errors for  $u$  in  $L^2$  and  $L^\infty$  norms.

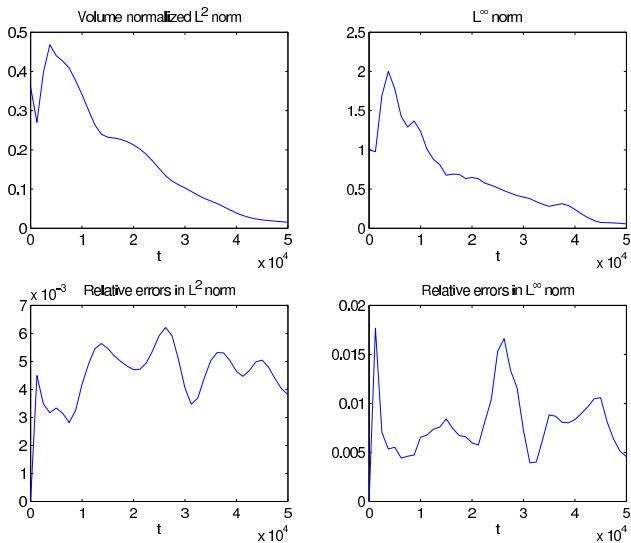


**FIGURE 35:** Top row: evolution of the solution  $v$  in  $L^2$  and  $L^\infty$  norms. Bottom row: evolution of the relative errors for  $v$  in  $L^2$  and  $L^\infty$  norms.

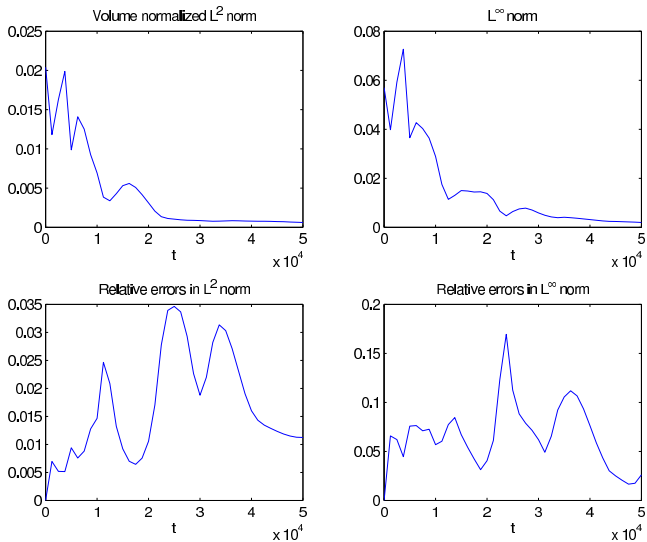


**FIGURE 36:** Top row: evolution of the solution  $w$  in  $L^2$  and  $L^\infty$  norms. Bottom row: evolution of the relative errors for  $w$  in  $L^2$  and  $L^\infty$  norms.

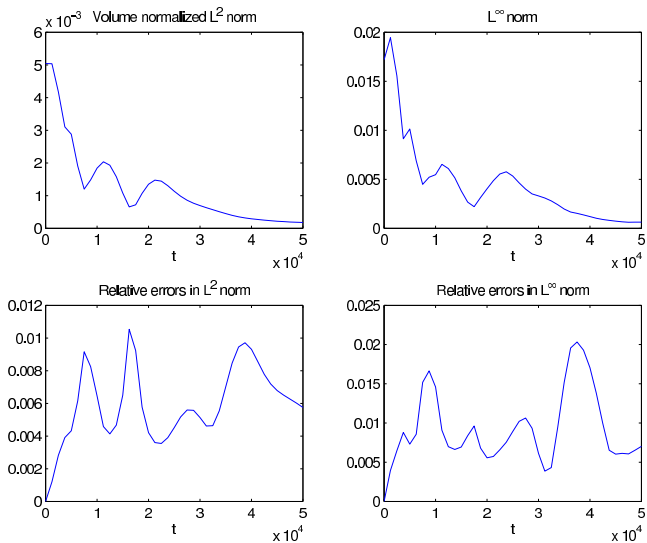


**FIGURE 37:** Top row: evolution of the solution  $\psi$  in  $L^2$  and  $L^\infty$  norms. Bottom row: evolution of the relative errors for  $\psi$  in  $L^2$  and  $L^\infty$  norms.

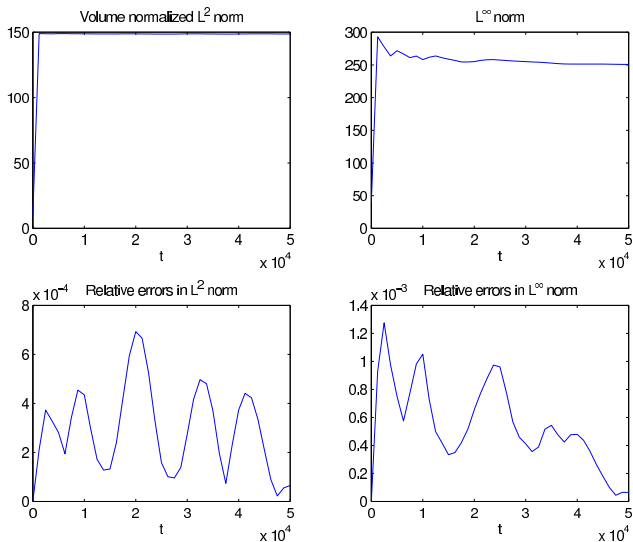


**FIGURE 38:** Top row: evolution of the solution  $\phi$  in  $L^2$  and  $L^\infty$  norms. Bottom row: evolution of the relative errors for  $\phi$  in  $L^2$  and  $L^\infty$  norms.

## Numerical Experiments

**Remark** *The relative errors for  $u$ ,  $v$ ,  $\psi$ , and  $\phi$  in both the  $L^2$  and  $L^\infty$  norms, are of the order of  $O(10^{-2})$ , and the relative errors for  $w$  are of the order of  $O(10^{-1})$ .*

## SUMMARY

- ▶ A new set of nonlocal boundary conditions has been implemented.
- ▶ We numerically verify that the proposed boundary conditions, proven suitable for the linearized equations, are also suitable for the nonlinear case.
- ▶ We numerically verify the transparency property of the proposed boundary conditions.

---

Inviscid PEs 2010.tex